

# Interaction Between Two Compressible, Turbulent Free Shear Layers

M. Samimy\*

*The Ohio State University, Columbus, Ohio*  
and

A. L. Addy†

*University of Illinois, Urbana, Illinois*

Experimental results of the interaction between two compressible, two-dimensional, turbulent free shear layers are presented. The shear layers were formed by geometrical separation of two high-Reynolds-number, turbulent boundary-layer flows with freestream Mach numbers of 2.07 and 1.50 from a 25.4-mm-high backward-facing step. A two-component, coincident laser Doppler velocimeter was utilized for a detailed flowfield survey. Both shear flows show general features similar to those of compressible, free shear layers reattaching onto a solid surface, including large-scale turbulence in the recompression and interaction regions and enhanced mixing in the redeveloping region. The free shear layer with the lower freestream Mach number shows high turbulence intensities and a higher rate of increase of turbulence intensities in the streamwise direction. These features appear to be caused by higher entrainment of reversed flow recirculating from the highly turbulent reattachment region.

## Introduction

THE work presented herein is part of an extensive research program to investigate recompression and reattachment of compressible, turbulent free shear layers and subsequent redeveloping boundary layers. The experimental efforts of this research have focused on simple, two-dimensional, backward-facing step geometries. These types of simple models, which have fixed separation points and contain all of the features of more general separated flows, have been widely used for many years in the investigation of subsonic and supersonic separated flows.<sup>1-9</sup>

Three different configurations were investigated in this research program in order to gain some basic knowledge about high-velocity separated flows. In the first configuration,<sup>6</sup> a Mach 2.46 flow with a turbulent boundary layer separated at a 25.4-mm step and formed a free shear layer that attached onto a ramp. The position and angle of the ramp were adjusted so that the incoming boundary layer separated at the step without any pressure change. The detailed turbulence results showed a gradual increase of turbulence intensities and shear stresses through the constant-pressure shear layer, a strong increase through the recompression and reattachment zone, and a gradual decrease after reattachment. This is in sharp contrast to incompressible shear-flow results, which show a sharp decay of turbulence intensity and shear stress upstream of the reattachment location. The maximum local turbulence intensities and shear stresses occurred around the sonic line in each transverse survey in disagreement with earlier hot-wire results,<sup>5</sup> which showed that these parameters peaked in the supersonic region of the shear layer. Large-scale turbulence near the lower edge of the shear layer in the reattachment region and enhanced mixing in the redeveloping boundary layer were detected, which confirmed earlier observations.<sup>4</sup>

In the second configuration,<sup>7</sup> a Mach 2.07 flow with a turbulent boundary layer separated at the step and subsequently formed a free shear layer that attached onto a flat plate parallel to the incoming boundary-layer flow direction (classic backstep geometry). The general trends of turbulence intensities and shear stresses were similar to those obtained in the first configuration with the exception of much higher fluctuation levels and higher anisotropy ratios. The differences appear to be caused by smaller size of the recirculating bubble and as a result a greater influence of the highly turbulent flow recirculating from the reattachment region. Also, the streamwise turbulence intensity increase through the separation at the step for the backstep experiment was a factor of approximately 1.3 higher than the ramp results. These results were in sharp contrast to the earlier observations by the schlieren technique<sup>10,11</sup> and measurements made by the hot-wire technique,<sup>12</sup> all of which showed a decay of the turbulence level through the expansion at the step. Some systematic experiments are needed to clarify this discrepancy.

The contributors to the measured fluctuations are the actual random turbulence fluctuations and the coherent large-scale oscillations. Since the time and length scales of the large-scale structures would be different for the two configurations, this could be another contributing factor to the observed different fluctuation levels in the ramp and backstep configurations.

In the third configuration, which is the subject of this paper, the interaction between two shear flows was investigated; see Fig. 1. The objective was the further exploration of compressible shear flows, specifically the effects of the interaction of shear flows with solid walls at reattachment on the turbulence scale and structure.

## Experimental Program

A series of dry, cold air experiments was conducted in a small-scale blowdown wind-tunnel facility. The wind-tunnel test-section width and height were 50.8 and 101.6 mm, respectively, and the step height was 25.4 mm; see Fig. 1. The approach Mach number, Reynolds number, stagnation pressure, and stagnation temperature were 2.07,  $5.85 \times 10^7/\text{m}$ , 457.3 kPa, and 295 K, respectively, for the upper boundary layer, and 1.50,  $3.37 \times 10^7/\text{m}$ , 233.8 kPa, and 295 K, respec-

Received Dec. 26, 1985; presented as Paper 86-0443 at the AIAA 24th Aerospace Sciences Meeting, Reno, NV, Jan. 6-9, 1986; revision received May 15, 1986. Copyright © American Institute of Aeronautics and Astronautics, Inc., 1986. All rights reserved.

\*Assistant Professor, Department of Mechanical Engineering, Member AIAA.

†Professor and Associate Head, Department of Mechanical and Industrial Engineering, Associate Fellow AIAA.

tively, for the lower boundary layer. The freestream Mach and Reynolds numbers after expansion at the step were 2.56 and  $3.98 \times 10^7/\text{m}$ , respectively, for the upper shear flow, and 2.23 and  $2.72 \times 10^7/\text{m}$ , respectively, for the lower shear flow. The Mach and Reynolds numbers of the upper free shear flow and two earlier configurations<sup>6,7</sup> were designed to be comparable for comparison of data.

For ease of presentation of the results, the dashed line in Fig. 1 is used to separate the upper and lower flows. The  $u$  velocity component direction was defined to correspond to the local freestream flow direction; parallel to the  $x$  coordinate for the incoming boundary-layer flows, rotated 12.4 deg relative to the  $x$  coordinate in a clockwise direction for the shear flow with higher  $M$ , and rotated 18.5 deg in the counterclockwise direction for the shear flow with lower  $M$ . The  $v$  velocity component is orthogonal to the corresponding  $u$  component in all cases.

A two-component, coincident laser Doppler velocimeter (LDV) system was used to make the velocity measurements. The details of data acquisition, reduction, and the errors involved have been reported earlier<sup>6,7</sup> and will not be repeated here. The LDV results reported here are corrected for velocity bias by using the two-dimensional velocity inverse weighting factor. The fringe bias correction was found to be unnecessary because a large focal-length lens was used in the highly turbulent region of the flowfield. Silicone oil particles with a mean diameter of approximately  $1 \mu\text{m}$  were used for seeding the flow. The errors due to the spatial resolution were less than 1% for the mean flow and 1.8% for the second-order fluctuation measurements. The statistical uncertainty due to a limited number of samples was better than  $\pm 2.8\%$  for the mean flow and  $\pm 3.2\%$  for the turbulence-intensity measurements.

## Experimental Results

### The Approach Boundary Layer

Two- and one-component velocity measurements were made to within 1 and 0.25 mm of the wall, respectively. The approach boundary-layer and momentum thicknesses for the Mach 2.07 and 1.5 boundary-layer flows were measured to be (2.26 and 0.18 mm) and (1.50 and 0.14 mm), respectively. The ratio of momentum thickness to boundary-layer thickness for the upper and lower flows was approximately 5 and 1%, respectively, higher than the values predicted by the method of Maise and McDonald.<sup>13</sup> Based on these and earlier results,<sup>6,7</sup> it appears that Maise and McDonald's prediction of the ratio of momentum to boundary-layer thickness for compressible turbulent boundary layers is in better agreement with experimental results at lower Mach numbers.

Figure 2 shows the boundary-layer, mean-velocity data of the present study in comparison with the Maise and McDonald curve.<sup>13</sup> The Mach 1.50 boundary-layer results

show better agreement with the curve than the Mach 2.07 results. The skin-friction coefficients  $C_f$  used in Fig. 2 were determined from the wall-wake law and were 0.00176 and 0.00247 for the upper and lower flows, respectively. These friction factors are in the range of values reported by Laderman<sup>14</sup> for comparable Mach and Reynolds numbers.

The boundary-layer, streamwise turbulence-intensity results for both flows show consistently higher values than those for the incompressible flow of Klebanoff,<sup>15</sup> but are in relatively good agreement with the data of Dimotakis et al.<sup>16</sup> at comparable Mach numbers. The boundary-layer, shear-stress results follow closely Sandborn's<sup>17</sup> "best estimate" for equilibrium compressible boundary layers.<sup>6</sup> The streamwise component of the skewness and flatness factors peak sharply at the outer edge of the boundary layers for both flows, then decline rapidly for the upper boundary layer and gradually for the lower boundary-layer flow. The Mach 2.85 turbulent boundary layers of Hayakawa et al.<sup>18</sup> and the Mach 2.43 results of Petrie et al.<sup>8</sup> showed skewness profiles similar to those of the Mach 2.07 flow of the present study.

### Two-Dimensionality of the Flowfield

All of the LDV data presented herein correspond to the centerline location of the wind tunnel. The uniformity of the mean flow and turbulence field across the tunnel was checked by additional LDV measurements at  $\pm 10$  mm on either side of the wind-tunnel centerline at  $x=28, 38$ , and  $46$  mm. The deviation of the data from the centerline values was the largest near the sonic line at  $x=28$  and  $38$  mm, where turbulence fluctuations were high as was the statistical uncertainty.<sup>6-8</sup> The maximum spanwise variation of the data for

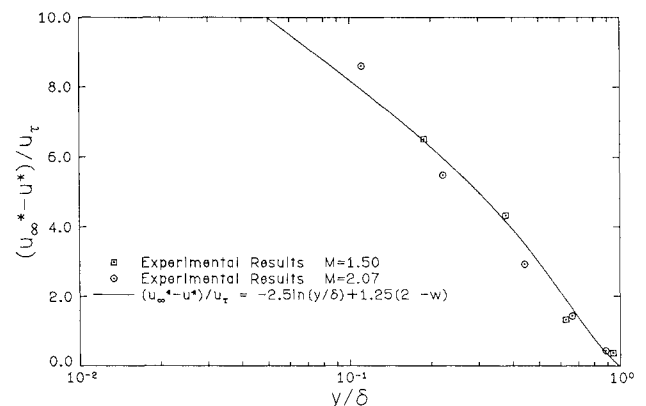


Fig. 2 Boundary-layer mean-velocity profiles and generalized curve of Maise and McDonald.<sup>13</sup>

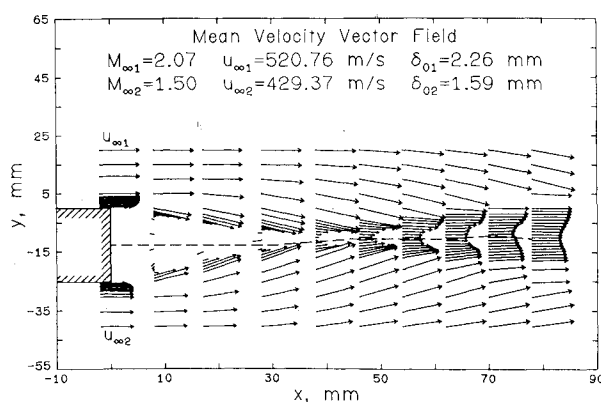


Fig. 1 Mean-velocity vector field.

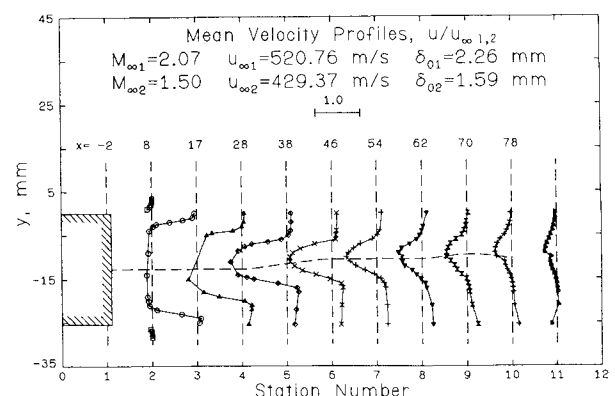


Fig. 3 Streamwise mean-velocity profiles ( $u_{\infty 1,2}$  means  $u_{\infty 1}$  for the higher-Mach-number flow and  $u_{\infty 2}$  for the lower-Mach-number flow).

the mean-velocity, streamwise turbulence intensity, and shear stress were  $\pm 1.9$ ,  $\pm 2.8$ , and  $\pm 2.5\%$ , respectively. These variations were within the statistical uncertainty for the finite sample size of the present experiments.<sup>6-8</sup> Since further off-center LDV measurements were not possible due to reflections of the laser light from the glass windows of the wind tunnel, it can only be concluded that the flow was two-dimensional within  $\pm 10$  mm of the centerline.

#### Mean Flow Results

The mean-velocity profiles for all measurement stations, including boundary-layer profiles, are shown in Fig. 3. The abscissa shows the station numbers, the vertical dashed lines indicate the location of zero velocity for each station, the numbers above the dashed lines give the  $x$  locations of the stations, and the horizontal dashed line chosen to separate the two shear flows for ease of presentation of the experimental results is also shown. The  $u$  velocity component direction was defined to correspond to the local freestream flow direction: parallel to the  $x$  coordinate, see Fig. 1, at station 1 for the incoming boundary-layer flows, rotated 12.4 deg in the clockwise direction for the higher-Mach-number shear flow, and 18.5 deg in the counterclockwise direction for the lower-Mach-number shear flow. The  $v$  velocity component is orthogonal to the corresponding  $u$  component. The velocities of higher and lower Mach number flows were non-dimensionalized by  $u_{\infty 1}$  and  $u_{\infty 2}$ , respectively, where  $u_{\infty 1}$  and  $u_{\infty 2}$  are the higher- and lower-Mach-number boundary-layer freestream velocities, respectively.

The mean-velocity results for both flows show similar trends up to the last three stations, where the velocity profiles exhibit a rapid "filling out." At the last three stations, the rate of profile development seems to be faster for the lower-Mach-number flow. This rapid development in the mean-velocity profiles has also been observed in redeveloping boundary layers.<sup>4,7</sup> Schlieren photographs of the present flowfield and earlier experiments<sup>7</sup> have shown the existence of large eddies stretched in the streamwise direction that seem to cause enhanced mixing in the redeveloping regions. This matter will be discussed further in the presentation of the turbulence field results.

#### Turbulence Field

The streamwise turbulence intensities for all stations are shown in Fig. 4. The maximum turbulence intensity at each station occurs near the sonic line for both shear flows. This is consistent with earlier LDV results<sup>6-8</sup> and disagrees with hot-wire results<sup>5</sup> that located the maximum in the supersonic region. For stations 3–7, the absolute maximum turbulence intensity at each station for the lower  $M$  flow is higher than that for the higher  $M$  flow and shows a faster streamwise growth. This could possibly be a Mach number effect, which means larger entrainment of recirculating flow coming from the highly turbulent interaction region, and/or due to the changes in the scales of coherent large-scale motions, which are one of the contributors of the measured fluctuations. The approximate location of the line separating forward and backward flows was determined to be at  $x = 35$  mm from oil streaks on the glass windows. For stations 8–10, the maximum turbulence intensity at each station for both flows spreads across the shear layer and also decays in the streamwise direction. An almost uniform turbulence-intensity profile across both shear layers at the last station confirms the existence of enhanced mixing in the redeveloping region, which was also observed by the rapid development of the mean-velocity profiles in Fig. 3.

The transverse turbulence-intensity profiles are shown in Fig. 5. For the first two stations after the expansion at the step, the maximum turbulence intensity occurs around the sonic line, which is similar to the streamwise turbulence intensity. Around the onset of interaction of the two shear flows and afterwards, the peak turbulence intensity occurs at

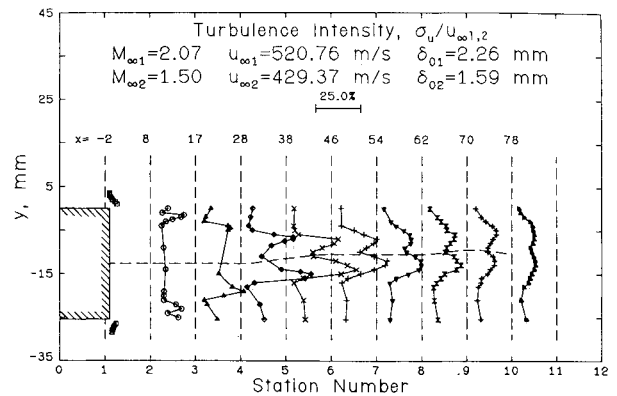


Fig. 4 Streamwise turbulence-intensity profiles.

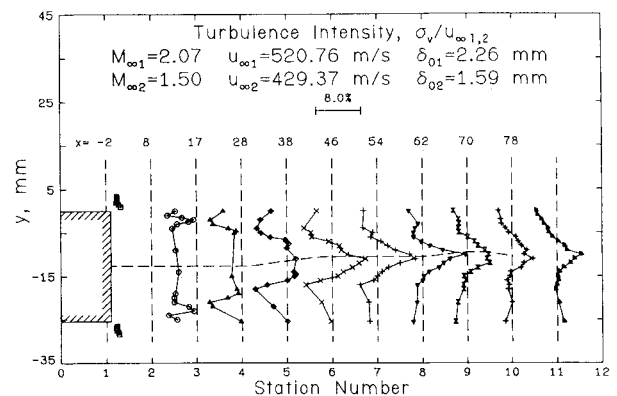


Fig. 5 Transverse turbulence-intensity profiles.

the interface region between the two flows, which shows high turbulence momentum exchange near the two flows. The anisotropy ratio  $\sigma_u/\sigma_v$  peaks near the sonic line for both flows and decays rapidly toward the interface between the two flows. As shown in Figs. 4–6, at the interface between the shear flows at the interaction region, the Reynolds shear stress is small and the anisotropy ratio is nearly unity. This type of turbulence is called isotropic turbulence in a crude sense.<sup>19</sup>

The evolutionary kinematic shear-stress profiles are shown in Fig. 6. The general trend, to some extent, is similar to the streamwise turbulence-intensity evolution; maximum stresses occur near the sonic line, very high shear stresses occur in the recompression and reattachment regions, and the absolute shear-stress level in the lower  $M$  flow is higher than in the higher  $M$  flow. The shear stress at the interface of the two shear flows is small, which is similar to the results for subsonic flows behind airfoils<sup>20</sup> and blunt bodies.<sup>21</sup> Growth of the maximum shear stress in both free shear layers in the streamwise direction and the existence of very large shear stresses near the onset of interaction of two shear flows in this study are consistent with earlier results where free shear layers attached onto solid surfaces.<sup>6,7</sup> This seems to indicate that imposition of the  $v=0$  boundary condition by the solid wall in the reattachment region does not affect turbulence intensity or scale in compressible reattaching shear flows. In contrast, for incompressible reattaching shear flows,<sup>1,22</sup> the  $v=0$  restriction is believed to be the cause of significant turbulence intensity and scale decay in the reattachment region. The convective velocity of large-scale motions in supersonic flows is higher than the local speed of sound.<sup>9</sup> Therefore, the large-scale structures are unaware of the existence of the solid walls. Thus, the breaking up process of the eddies perhaps would occur at or after reattachment. This could be a cause for the differences between subsonic and supersonic reattaching shear flows.

The axial distributions of the maximum turbulence intensities and kinematic shear stresses are shown in Fig. 7. The general trends are the same for both shear flows and similar to earlier results.<sup>6,7</sup> The plateau in maximum turbulence intensities in compressible flows occurs in the reattachment region, while the same type of plateau has been observed in incompressible flow about one step height before reattachment. The rate of increase of the turbulence intensity and shear stress is higher for the shear flow with the lower freestream Mach number. The growth rate of those compressible shear layers is approximately a factor of 2 or more less than the average incompressible results.<sup>6-8</sup> For compressible shear flows, previous work has shown that the growth rate is inversely proportional to Mach number,<sup>23,24</sup> which is consistent with the present results in that the lower-Mach-number shear-layer growth and entrainment rate are higher. The entrained recirculating flow coming from the highly turbulent reattachment region could be “charging up” the turbulence field of the lower shear flow, thus causing higher turbulence intensity and shear stress. Another possible cause could be the larger distortion of the turbulence field passing through the 18.5-deg expansion at the step for the lower  $M$  flow in comparison to the higher  $M$  flow with only a 12.4-deg expansion.

The ratio of the kinematic shear stress to the estimated turbulent kinetic energy is shown in Fig. 8, where  $k$  is estimated to be equal to  $\frac{3}{4}(\sigma_u^2 + \sigma_v^2)$ . Harsha and Lee<sup>25</sup> examined this parameter for boundary layers, two-dimensional and circular jets, and wakes in incompressible flow. They concluded that a value of 0.3 for this parameter is reasonable for computational purposes. Bradshaw and Ferriss<sup>26</sup> and Bradshaw<sup>27</sup> also assumed a value of 0.3 for this parameter in their compressible boundary-layer calculations. This parameter, which is often called the turbulence “structure parameter,” generally does not vary significantly but, as

is seen in Fig. 8, the variation in this flowfield is significant. Another turbulence “structure parameter,” the shear-stress correlation coefficient defined as  $u'v'/\sigma_u\sigma_v$ , showed a similar trend thus confirming significant turbulence structural changes in the flowfield.

Figures 9 and 10 show two components of the turbulence triple products. The results show significant increases in the triple products, which most probably means an increase in turbulence scale in the recompression and interaction regions. This is similar to results obtained in free shear layers reattaching to a solid wall, and it may be interpreted that solid boundaries in the reattachment region do not have a significant impact on the turbulence scale and turbulence intensities, Fig. 7. This is in contrast to speculation about the significant effects of solid walls at reattachment on turbulence characteristics in subsonic flows.<sup>1,22</sup> As discussed

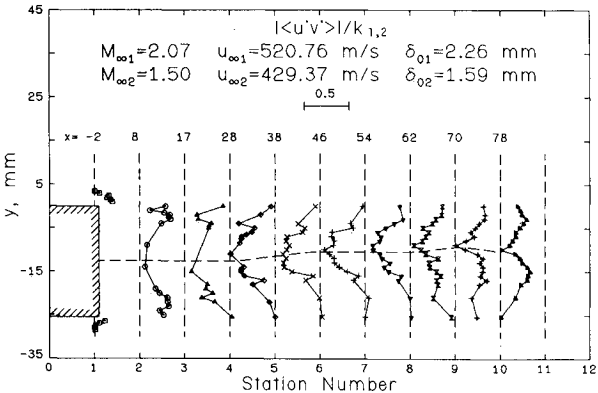


Fig. 8 Turbulence “structure parameter” profiles.

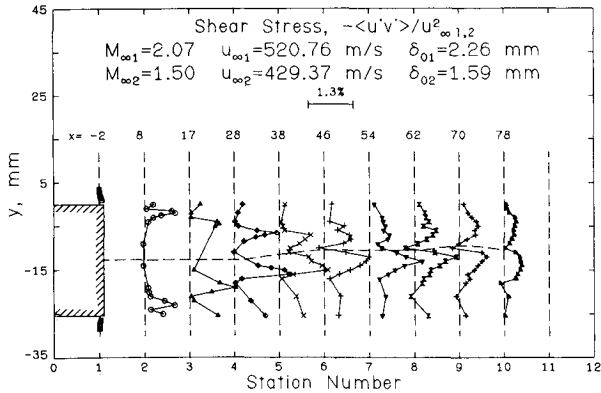


Fig. 6 Evolutionary shear-stress profiles.

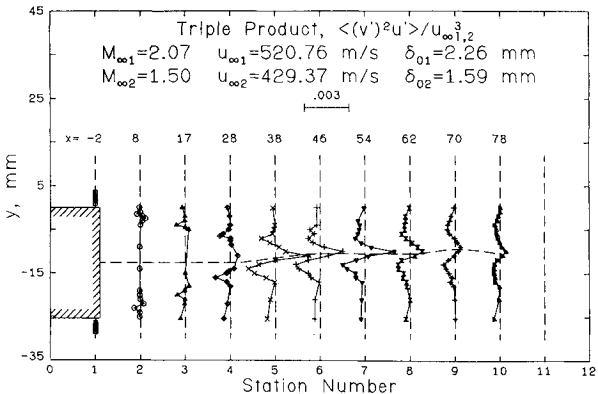


Fig. 9 Turbulent triple product.

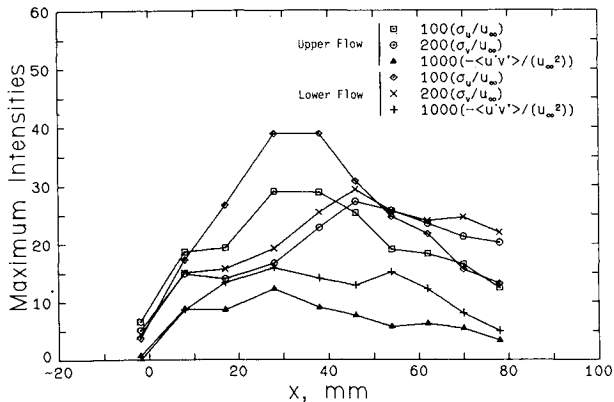


Fig. 7 Maximum turbulence fluctuations and shear stresses.

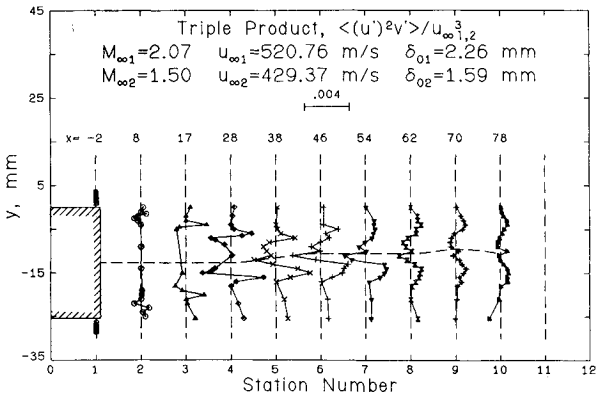


Fig. 10 Another component of the turbulent triple product.

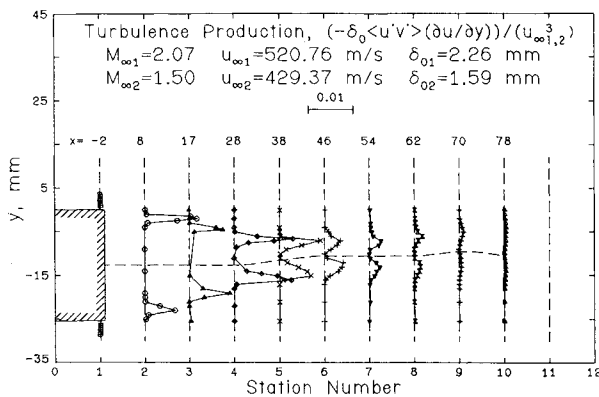


Fig. 11 Turbulence production.

earlier, the high convective velocity of large-scale eddies in supersonic shear flows could be a cause for these differences.

Two components of the triple products—namely,  $\langle (v')^2 u' \rangle$ , Fig. 9, and  $\langle (u')^3 \rangle$ —show behavior in the transverse direction similar to that of incompressible shear flows.<sup>1,22</sup> This suggests similar streamwise turbulence diffusion characteristics in incompressible and compressible shear layers. The significant difference between incompressible and compressible shear flows occurs in the  $\langle (u')^2 v' \rangle$  and  $\langle (v')^3 \rangle$  components of the triple products, which is related to the diffusion of turbulence in the transverse direction. In compressible shear flows, see Fig. 10, in the lower edge of both shear flows and also in the interaction region, turbulence diffusion is inward (toward the wind-tunnel centerline) and in the upper edges of the shear flow it is outward (away from the wind-tunnel centerline). This is opposite to incompressible shear-flow cases and seems to be a significant structural difference.

Figure 11 shows kinematic turbulence production, which excludes significant density changes through the recompression and interaction regions. Turbulence production is high in developing shear flows, which is similar to subsonic reattaching shear flows<sup>22</sup> and other compressible reattaching shear flows.<sup>6,28</sup> However, this high level of production in the recompression and onset of interaction regions have not been observed in incompressible flows. The dramatic decay of turbulence production in the redeveloping region is obviously caused by the rapid development of the mean-velocity profiles in this region, which confirms the existence of enhanced mixing and is consistent with earlier results.<sup>28</sup>

### Conclusions

Detailed experimental results of the interaction between two free shear layers utilizing a two-component, coincident laser Doppler velocimeter have been documented. The general trends for both shear layers are the same and similar to those of compressible shear layers reattaching to solid surfaces. Therefore, in contrast to incompressible reattaching shear layers, where imposition of the  $v=0$  restriction by the solid surface at the reattachment location is believed to decrease significantly the turbulence scale and intensities, this does not appear to be the case for compressible shear flows. In addition, the results have confirmed earlier findings of essential structural difference between compressible and incompressible shear flows, especially in terms of the diffusion of turbulence energy in the transverse direction. The turbulence-intensity levels and rate of increase in the streamwise direction in the shear layer with the lower Mach number were higher. This could be caused by a higher entrainment rate of highly turbulent recirculating flow, and/or by contribution from the large-scale structures.

### Acknowledgment

This research was supported by the U.S. Army Research Office, Dr. Robert E. Singleton, Contract Monitor.

### References

- Eaton, J.K. and Johnston, J.P., "A Review of Research on Subsonic Turbulent Flow Reattachment," *AIAA Journal*, Vol. 19, Sept. 1981, pp. 1093-1100.
- Chapman, D.R., "An Analysis of Base Pressure at Supersonic Velocities and Comparison with Experiment," NACA TN 2137, 1950.
- Roshko, A. and Thomke, G.J., "Observations of Turbulent Reattachment Behind an Axisymmetric Downstream-Facing Step in Supersonic Flow," *AIAA Journal*, Vol. 4, June 1966, pp. 975-980.
- Settles, G.S., Baca, B.K., Williams, D.R., and Bogdonoff, S.M., "A Steady of Reattachment of a Free Shear Layer in Compressible, Turbulent Flow," *AIAA Journal*, Vol. 20, Jan. 1982, pp. 60-67.
- Hayakawa, K., Smits, A.J., and Bogdonoff, S.M., "Turbulence Measurements in a Compressible Reattaching Shear Layer," *AIAA Journal*, Vol. 22, July 1984, pp. 889-895.
- Samimy, M., Petrie H.L., and Addy, A.L., "A Study of Compressible Turbulent Reattaching Free Shear Layers," *AIAA Journal*, Vol. 24, Feb. 1986, pp. 261-267.
- Samimy, M., Petrie, H.L., and Addy, A.L., "Reattachment and Redevelopment of Turbulent Free Shear Layers," *International Symposium on Laser Anemometry*, ASME, New York, FED Vol. 33, 1985, pp. 159-166.
- Petrie, H.L., Samimy, M., and Addy, A.L., "A Study of Compressible Turbulent Free Shear Layers Using Laser Doppler Velocimetry," AIAA Paper 85-0177, 1985; also, to appear in *AIAA Journal*.
- Ikawa, H. and Kubota, T., "Investigation of Supersonic Turbulent Mixing Layer with Zero Pressure Gradient," *AIAA Journal*, Vol. 13, May 1975, pp. 566-572.
- Page, R.H. and Sernas, V., "Apparent Reverse Transition in an Expansion Fan," *AIAA Journal*, Vol. 8, Jan. 1970, pp. 189-190.
- Small, R.D. and Page, R.H., "Turbulent Supersonic Boundary Layer Flow in the Neighborhood of a 90° Corner," *Astronautica Acta*, Vol. 18, Feb. 1973, pp. 99-107.
- Lewis, J.E. and Behrens, W., "Fluctuation Measurements in the Wake With and Without Base Injection," *AIAA Journal*, Vol. 7, April 1969, pp. 664-670.
- Maise, G. and McDonald, H., "Mixing Length and Kinematic Eddy Viscosity in a Compressible Boundary Layer," *AIAA Journal*, Vol. 6, Jan. 1968, pp. 73-80.
- Laderman, A.J., "Adverse Pressure Gradient on Supersonic Boundary Layer Turbulence," *AIAA Journal*, Vol. 18, Oct. 1980, pp. 1186-1195.
- Klebanoff, D.S., "Characteristics of Turbulence in a Boundary Layer with Zero Pressure Gradient," NACA Rept. 1247, 1955.
- Dimotakis, P.E., Collins, D.J., and Lang, D.B., "Laser Doppler Measurements in Subsonic, Transonic, and Supersonic Turbulent Layers," *Laser Velocimetry and Particle Sizing*, edited by H.D. Thompson and W.H. Stevenson, Hemisphere Publishing Co., New York, 1979, pp. 208-219.
- Sandborn, V.A., "A Review of Turbulence Measurements in Compressible Flow," NASA TM X-62-337, March 1974.
- Hayakawa, K., Smits, A.J., and Bogdonoff, S.M., "Hot-Wire Investigation of an Unseparated Shock-Wave/Turbulent Boundary-Layer Interaction," *AIAA Journal*, Vol. 22, May 1984, pp. 579-585.
- Townsend, A.A., *The Structure of Turbulent Shear Flow*, 2nd Ed., Cambridge University Press, New York, 1976.
- Andreopoulos, J. and Bradshaw, P., "Measurements of Interacting Turbulent Shear Layers in the Near Wake of a Flat Plate," *Journal of Fluid Mechanics*, Vol. 100, Pt. 3, 1980, pp. 639-668.
- Palmer, M.D. and Keffer, J.F., "An Experimental Investigation of an Asymmetrical Turbulent Wake," *Journal of Fluid Mechanics*, Vol. 53, Pt. 4, 1972, pp. 593-610.
- Chandrsuda, C. and Bradshaw, P., "Turbulence Structure of a Reattaching Mixing Layer," *Journal of Fluid Mechanics*, Vol. 110, 1981, pp. 171-194.

<sup>23</sup>Channapragada, R.S., "Compressible Jet Spread Parameter for Mixing Zone Analysis," *AIAA Journal*, Vol. 1, Sept. 1963, pp. 2188-2190.

<sup>24</sup>Birch, S.F. and Eggers, J.M., "A Critical Review of the Experimental Data for Developed Free Turbulent Shear Layers," *Free Turbulent Shear Flows*, Vol. 1, NASA SP-321, 1972.

<sup>25</sup>Harsha, P.T. and Lee, S.C., "Correlation Between Turbulent Shear Stress and Turbulent Kinetic Energy," *AIAA Journal*, Vol. 8, Aug. 1970, pp. 1508-1510.

<sup>26</sup>Bradshaw, P. and Ferriss, D.H., "Calculation of Boundary Layer Development Using the Turbulent Energy Equation: Com-

pressible Flow on Adiabatic Walls," *Journal of Fluid Mechanics*, Vol. 46, Pt. 1, 1971, pp. 83-110.

<sup>27</sup>Bradshaw, P., "Mean Compression Effects in Turbulent Boundary Layers," *Journal of Fluid Mechanics*, Vol. 63, Pt. 3, 1974, pp. 449-464.

<sup>28</sup>Gaviglio, J., Dussauge, J.P., Debieve, J.F., and Favre, A., "Behavior of a Turbulent Flow Strongly Out of Equilibrium at Supersonic Speeds," *The Physics of Fluids*, Vol. 20, No. 10, Pt. 2, 1977, pp. 5179-5192.

*From the AIAA Progress in Astronautics and Aeronautics Series...*

## **FUNDAMENTALS OF SOLID-PROPELLANT COMBUSTION — v. 90**

*Edited by Kenneth K. Kuo, The Pennsylvania State University  
and  
Martin Summerfield, Princeton Combustion Research Laboratories, Inc.*

In this volume distinguished researchers treat the diverse technical disciplines of solid-propellant combustion in fifteen chapters. Each chapter presents a survey of previous work, detailed theoretical formulations and experimental methods, and experimental and theoretical results, and then interprets technological gaps and research directions. The chapters cover rocket propellants and combustion characteristics; chemistry ignition and combustion of ammonium perchlorate-based propellants; thermal behavior of RDX and HMX; chemistry of nitrate ester and nitramine propellants; solid-propellant ignition theories and experiments; flame spreading and overall ignition transient; steady-state burning of homogeneous propellants and steady-state burning of composite propellants under zero cross-flow situations; experimental observations of combustion instability; theoretical analysis of combustion instability and smokeless propellants.

For years to come, this authoritative and compendious work will be an indispensable tool for combustion scientists, chemists, and chemical engineers concerned with modern propellants, as well as for applied physicists. Its thorough coverage provides necessary background for advanced students.

*Published in 1984, 891 pp., 6 × 9 illus. (some color plates), \$59.50 Mem., \$89.50 List; ISBN 0-915928-84-1*

**TO ORDER WRITE: Publications Order Dept., AIAA, 1633 Broadway, New York, N.Y. 10019**